

# Microtubule Dynamics in Living Root Hairs: Transient Slowing by Lipochitin Oligosaccharide Nodulation Signals <sup>W</sup>

Valya N. Vassileva,<sup>a,1</sup> Hiroshi Kouchi,<sup>b</sup> and Robert W. Ridge<sup>a,2</sup>

<sup>a</sup>Department of Biology, Division of Natural Sciences, International Christian University, Mitaka-shi, 181-8585 Tokyo, Japan

<sup>b</sup>Department of Plant Physiology, National Institute of Agrobiological Sciences, Tsukuba, Ibaraki 305-8602, Japan

**The incorporation of a fusion of green fluorescent protein and tubulin- $\alpha$  6 from *Arabidopsis thaliana* in root hairs of *Lotus japonicus* has allowed us to visualize and quantify the dynamic parameters of the cortical microtubules in living root hairs. Analysis of individual microtubule turnover in real time showed that only plus polymer ends contributed to overall microtubule dynamicity, exhibiting dynamic instability as the main type of microtubule behavior in *Lotus* root hairs. Comparison of the four standard parameters of in vivo dynamic instability—the growth rate, the disassembly rate, and the frequency of transitions from disassembly to growth (rescue) and from growth to disassembly (catastrophe)—revealed that microtubules in young root hairs were more dynamic than those in mature root hairs. Either inoculation with *Mesorhizobium loti* or purified *M. loti* lipochitin oligosaccharide signal molecules (Nod factors) significantly affected the growth rate and transition frequencies in emerging and growing root hairs, making microtubules less dynamic at a specific window after symbiotic inoculation. This response of root hair cells to rhizobial Nod factors is discussed in terms of the possible biological significance of microtubule dynamics in the early signaling events leading to the establishment and progression of the globally important Rhizobium/legume symbiosis.**

## INTRODUCTION

Microtubules are dynamic polymers that play a prominent role in plant morphogenesis and cellular organization. Their dynamics consist mainly of stochastic phases of polymerization and disassembly, a pattern of behavior known as dynamic instability (Mitchison and Kirschner, 1984), which can be defined in terms of growth, disassembly, the transition from growth to disassembly (catastrophe), and the transition from disassembly to growth (rescue; Hush et al., 1994; Dhonukshe and Gadella, 2003; Vos et al., 2003a). By changes in these dynamic instability parameters, cells rearrange the microtubular network and quickly respond to environmental and developmental stimuli (Desai and Mitchison, 1997). The cellular function of microtubules critically depends on their intrinsic polarity, defined by a fast-growing plus end and a more stable minus end. In most eukaryotes, microtubules are nucleated within the microtubule-organizing center to which their minus ends are usually attached (Wade and Hyman, 1997; Erhardt et al., 2002; Schmit, 2002). When the minus end is not anchored at the microtubule-organizing center, the continual addition of subunits at the plus ends equals the

disassembly at the opposite minus ends, a behavior termed treadmilling (Margolis and Wilson, 1978). Recently, in vivo imaging of individual microtubules revealed a hybrid treadmilling mechanism in the cortex of epidermal cells of *Arabidopsis thaliana* (Shaw et al., 2003). This mechanism is characterized by polymerization-biased dynamic instability at the plus ends and slow depolymerization at the minus ends.

Plant cells possess cortical microtubules that are organized into ordered arrays (Williamson, 1991; Cyr, 1994; Goddard et al., 1994). In root hairs, cortical microtubules present in all stages of root hair development, in stage-specific configurations (Sieberer et al., 2002; Van Bruaene et al., 2004). Experiments with microtubule depolymerizing and stabilizing drugs have shown that cortical microtubules are involved in regulating the directionality and stability of apical growth in root hairs (Bibikova et al., 1999). During the establishment of the symbiotic association between legume plants and rhizobia, the microtubule cytoskeleton assists in the infection process, as well as in the differentiation and maintenance of root nodules, in which nitrogen fixation takes place (Ridge, 1992; Timmers et al., 1998; Catoira et al., 2001). One of the most prominent events in the infection process is root hair curling around bacteria that leads to the formation of an infection thread within the root hair. Generally, microtubules are abundant at the site of infection thread initiation and along the infection thread body (Ridge and Rolfe, 1985). They surround the host cell nucleus and apparently connect it to both the root hair tip and the growing infection thread tip (Timmers et al., 1999). A recent study by Weerasinghe et al. (2003) reported that application of *Rhizobium meliloti* Nod factors caused rapid and dynamic changes of the pattern of microtubules in chemically fixed root hairs of *Medicago sativa*. Lipochitin oligosaccharide Nod factors, produced by rhizobia, are communication signals that mediate

<sup>1</sup> Current address: Academic Metodi Popov Institute of Plant Physiology, Bulgarian Academy of Sciences, Academic Georgi Bonchev Street, Block 21, 1113 Sofia, Bulgaria.

<sup>2</sup> To whom correspondence should be addressed. E-mail rwr@ic.u.ac.jp; fax 81-422-331-449.

The author responsible for distribution of materials integral to the findings presented in this article in accordance with the policy described in the Instructions for Authors ([www.plantcell.org](http://www.plantcell.org)) is: Robert W. Ridge (rwr@ic.u.ac.jp).

<sup>W</sup>Online version contains Web-only data.

Article, publication date, and citation information can be found at [www.plantcell.org/cgi/doi/10.1105/tpc.105.031641](http://www.plantcell.org/cgi/doi/10.1105/tpc.105.031641).

the molecular dialog between the legume plant and its bacterial partner (Spaenk, 2000). Most of the responses of root hairs to bacterial inoculation can be seen by the application of purified Nod factors that permits an experimental analysis of the early events leading to symbiosis establishment (de Ruijter et al., 1998; Niwa et al., 2001). A transient depolymerization of microtubular cytoskeleton and recovery thereafter have been reported in root hairs of *Medicago* plants after exposure to purified *R. meliloti* Nod factors (Weerasinghe et al., 2003).

All these observations of the root hair microtubular network have been done only by conventional techniques based on chemical fixation. The possibility for visualizing microtubules in fixed cells by immunofluorescence and electron microscopy is rather limited because it does not allow in vivo observation and quantification of the dynamics of microtubules. Green fluorescent protein (GFP) isolated from the jellyfish *Aequorea victoria* has enabled real-time in vivo visualization of cytoskeletal dynamics within a variety of eukaryotic systems, including higher plants, without causing any perceptible tissue damage (Chalfie et al., 1994; Haseloff and Amos, 1995; Haseloff et al., 1997).

So far, there are only very few reports on the microtubule architecture in living root hairs of plants, transformed with GFP (Sieberer et al., 2002; Vos et al., 2003b; Van Bruaene et al., 2004). These studies are mainly focused on the observation of microtubules in transgenic plants, expressing GFP-microtubule binding domain (GFP-MBD) fusion protein. However, there have been no detailed analyses and quantification of the dynamic parameters of cortical microtubules in living root hair cells.

In this study, as an experimental approach to understanding the dynamic turnover of cortical microtubules in living root hairs, transgenic lines of the model legume *Lotus japonicus* that stably express a fusion protein of GFP and tubulin- $\alpha$  6 (GFP-TUA6) from *Arabidopsis* were used. The GFP-TUA6 fusion construct has been successfully used to label the distribution patterns of microtubules in *Arabidopsis* leaf and hypocotyl cells (Ueda et al., 1999) and in epidermal cells of cotyledons of *Arabidopsis* after attack by oomycete pathogens (Takemoto et al., 2003). In this study, the GFP-TUA6 labeling has revealed the configuration and dynamics of the cortical microtubular network in *L. japonicus* root hair cells during the earliest stages of forming a beneficial symbiotic relationship with *Mesorhizobium loti*. We quantified and compared the four standard parameters of dynamic instability (microtubule growth rate, microtubule disassembly rate, and the transition frequencies between these states) in root hairs of uninoculated plants, plants inoculated with *M. loti* TONO, and plants inoculated with purified *M. loti* Nod factors. Using time-lapse series of confocal images acquired from different developmental zones of root hairs, we demonstrate significant changes in microtubule organization and some of the parameters of dynamic instability after Nod factor application.

## RESULTS

### Transgenic Plants and GFP Expression in Root Hair Cells

*L. japonicus* B-129 Gifu plants were transformed with a translational fusion GFP and TUA6 from *Arabidopsis* (Ueda et al.,

1999) under the control of a 35S promoter of *Cauliflower mosaic virus*. Five of the transgenic lines showed strong and stable expression of GFP in cortical microtubules in leaf and hypocotyl epidermis at the T2 generation. Genomic DNA gel blot hybridization with TUA6 cDNA as a probe indicated that these lines contained multiple transgene copies (data not shown). Microtubules in the root hair cells were clearly recognized in three of the lines, but in two other lines, GFP fluorescence mostly remained in the cytoplasm of the root hair cells and was not well integrated into microtubules. One of the selected lines, 5C, that exhibited stable GFP-TUA6 fluorescence of microtubules in root hair cells was chosen for further analysis. We were able to observe highly patterned arrays of cortical microtubules in root (Figure 1A), root hair (Figures 1B to 1E), as well as in hypocotyl and leaf epidermal cells, showing that the decoration with GFP-TUA6 has enabled us to visualize microtubules in all plant tissues without any aberrant microtubule organization patterns. In addition, we did not observe any defects in the growth, flowering, and seed production of the GFP-TUA6 transgenic plants.

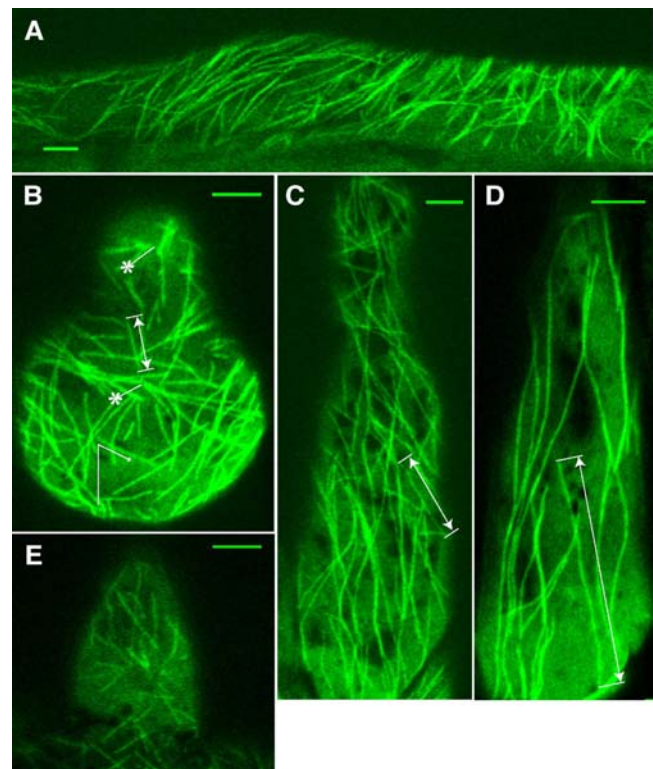


**Figure 1.** Visualization of Cortical Microtubules in *L. japonicus* Plants Transformed with GFP-TUA6.

- (A) Root epidermal cell.  
 (B) Emerging (Zone I) root hair cell. Asterisks indicate the sites of microtubule nucleation.  
 (C) Growing (Zone II) root hair cell.  
 (D) Mature (Zone III) root hair cell.  
 (E) Emerging (Zone I) root hair cell of 10-d-old *Lotus* plant. Sample measurements of microtubule length [(B) to (D)], double-sided arrows and angles [(B), arrow]. Bars = 5  $\mu$ m.

Analysis of variance (ANOVA;  $P > 0.05$ ) has shown that the average growth rate of root hairs of GFP-TUA6 transgenic plants ( $0.84 \pm 0.32 \mu\text{m}/\text{min}$ , mean  $\pm$  SE,  $n = 24$ ) was not significantly different from the growth rates of root hairs of control Gifu plants ( $1.16 \pm 0.39 \mu\text{m}/\text{min}$ , mean  $\pm$  SE,  $n = 26$ ).

Observation by confocal laser scanning microscopy revealed GFP-labeled microtubules during all stages of root hair development (Figures 1B to 1D), but the intensity of GFP fluorescence varied considerably between the growth stages of the plants and root hairs. Generally, in young plants (4 to 7 d old), GFP fluorescence was strong and microtubules in root hair cells could be seen easily (Figures 1A to 1D), whereas older plants often exhibited a low level of fluorescence and microtubules could not clearly be seen even in young root hair cells (Figure 1E). In addition, GFP fluorescence tended to decrease in the basipetal direction of the root hairs and appeared less bright in mature root hairs than in the young ones.

### Root Hair Zonation and Organization of Cortical Microtubules

The detailed comparison of cortical microtubule patterns throughout different developmental stages of root hairs (Figures 1B to 1D) allowed us to identify three successive root hair zones: Zone I, containing emerging and short growing root hairs with a length of 10 to 40  $\mu\text{m}$ ; Zone II, where medium length (from 40 to 90  $\mu\text{m}$ ) root hairs were actively growing; and Zone III, containing fully grown mature root hairs (with a length  $> 90 \mu\text{m}$ ). In vivo measurement of root hair growth showed that the characteristic growth rates of root hairs from these successive developmental zones differed significantly ( $P > 0.001$ ) amongst themselves (Figure 2). Root hairs of Zone I exhibited average growth rates of  $0.34 \pm 0.12 \mu\text{m}/\text{min}$ , which were much lower than those determined for Zone II root hairs ( $1.27 \pm 0.31 \mu\text{m}/\text{min}$ ). Mature root hairs examined showed distinct cessation of their tip growth.

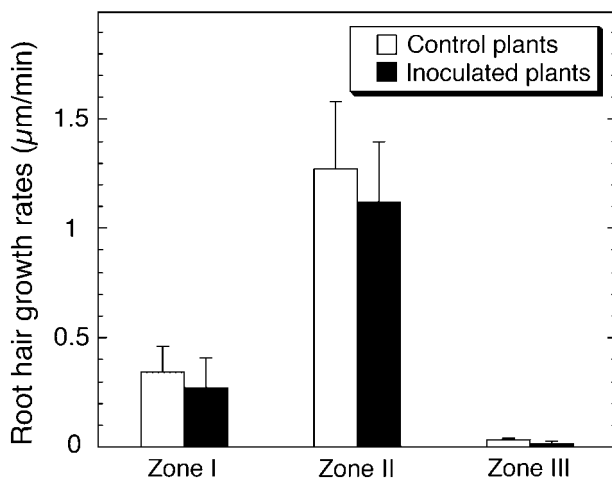


**Figure 2.** Average Growth Rates of *L. japonicus* Root Hairs at Different Stages of Their Development.

Vertical bars represent the standard errors of the means ( $n = 95$ ).

Each stage of root hair development showed a specific organization of cortical microtubules (Figures 1B to 1D). The classification of microtubules was done according to their length and angles of orientation with respect to the longitudinal axis of root hairs. To quantify microtubule length, we measured single microtubules with both visible ends in the field of view (Figures 3A and 3B). In many time-lapse movies, however, the bundled nature of microtubules (Figures 4A to 4D, asterisks) prevented the observation of single microtubules. In this case, we measured the length of overlapped and bundled microtubule structures (see supplemental data online). On average, the bundled microtubules seemed to be longer than the single ones that could be explained by the microtubule overlapping. However, the tendency for microtubule length distributions in different root hair zones remained unchanged. That is why, for the length analysis, we selected mainly unbundled microtubules (Figures 3A and 3B), whose quantification was considered as more accurate.

Zone I was characterized by the presence of short microtubules (up to 15  $\mu\text{m}$  in length, Figure 3A) with random arrangement (all orientations occurred almost at the same frequency; Figure 3C). Growing (Zone II) root hairs contained cortical microtubules with a highly variable length and orientation (Figures 3A and 3C). In the base part of root hairs, most microtubules ( $>60\%$ ) were relatively long (from 15 to 30  $\mu\text{m}$ ; Figure 3B) and axially oriented (Figure 3D), but in the tip part, they tended to be shorter (with a length of 1 to 15  $\mu\text{m}$ , Figure 3B) and with a larger deviation from the main root hair axis (Figure 3D). The tip of the emerging and growing root hairs was very often devoid of microtubules (Figure 1B).

In Zone III, long microtubules (15 to 30  $\mu\text{m}$  in length; Figure 3A) with longitudinal orientation (Figure 3C) were predominant. Their relative abundance was highly decreased, and they appeared very often as thick microtubule strands (Figure 1D).

### Microtubule Dynamic Instability in Lotus Root Hair Cells

Wherever both ends of a microtubule were visible, time-lapse image recording of microtubule dynamics showed that one end (conventionally termed the plus end) was very dynamic in that it underwent random phases of growth and disassembly, whereas the other end (the minus end) did not (Figures 4A to 4D). Therefore, cortical microtubules in root hairs of *Lotus* plants exhibited dynamic instability behavior. The plus ends of adjacent microtubules were often oriented in various directions (Figures 4A to 4D), revealing that this aspect of the organization of cortical microtubules in root hairs was not polarized. The arrows in Figure 5 point to the dynamic plus end of a single microtubule in root hair of Zone I. As seen by the selected frames (Figure 5) from a time-lapse movie (see Supplemental Video 1 online), this microtubule displayed variable periods of growth (0 to 20 s and 116 to 140 s; arrows), pausing (32 to 44 s; arrowheads), or disassembly (64 to 104 s; double arrows). Asterisks in the same figure indicate a rare event: a microtubule breakage. The newly formed ends that behaved like plus ends were immediately depolymerized (44 to 76 s) and after that polymerized again (104 to 140 s).

By examining the four basic parameters of dynamic instability—the rates of microtubule growth and disassembly and the transition frequencies from disassembly phase to growth

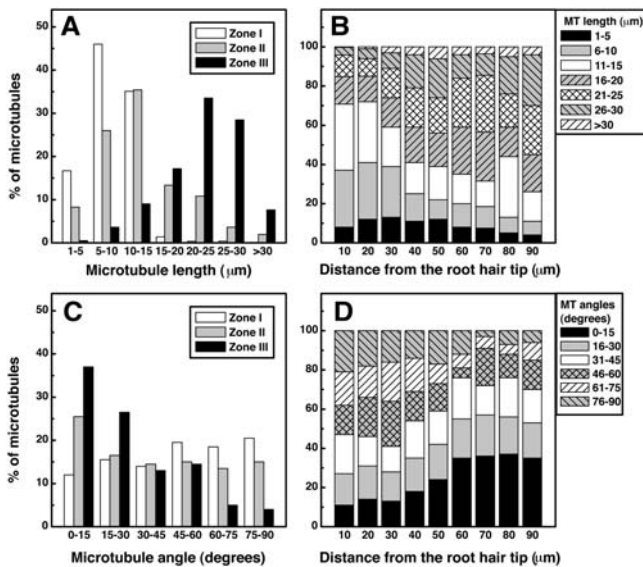


**Figure 3.** Cortical Microtubule Arrangement of *L. japonicus* Root Hairs at Different Stages of Their Development.

(A) Average microtubule length ( $n = 952$  microtubules from 136 root hairs).

(B) Microtubule length in Zone II root hairs as a function of distance from root hair tip ( $n = 504$  microtubules from 63 root hairs).

(C) Average microtubule angular orientation ( $n = 1518$  microtubules from 138 root hairs).

(D) Microtubule angular orientation in Zone II root hairs as a function of distance from root hair tip ( $n = 858$  microtubules from 78 root hairs).

phase (rescue) and from growth phase to disassembly phase (catastrophe)—we compared the main dynamic properties of microtubules from different root hair zones (Table 1). Microtubule growth in emerging and growing root hairs occurred at mean rates of  $4.62 \pm 0.16 \mu\text{m}/\text{min}$  and  $4.48 \pm 0.38 \mu\text{m}/\text{min}$ , respectively. These rates were significantly higher ( $P < 0.001$ ) than the mean rates measured for microtubules in mature root hairs ( $3.11 \pm 0.12 \mu\text{m}/\text{min}$ ). However, we could not find any significant differences in disassembly rates between different root hair zones (Table 1). Microtubule dynamics in Lotus root hair cells were also characterized by asymmetric transition frequency, with a high rescue frequency and a low catastrophe frequency (Table 1). Rescue events, observed in Zone I and Zone II root hairs, were respectively 380 and 420% more frequent than catastrophe events. In mature root hairs, the rescue frequency was  $\sim 70\%$  lower than that observed in emerging and growing root hairs (Table 1). Catastrophe events occurred at a frequency of  $1.38 \pm 0.17$  events/min and were 42% less frequent than rescue events, which were observed at a frequency of  $2.39 \pm 0.22$  events/min.

### Organization of Cortical Microtubules in Rhizoid and Nod Factor-Treated Plants

The most obvious response of Lotus plants to inoculation with purified *M. loti* Nod factors was induction of numerous root hair

deformations in the form of curled (Figure 6A), branched (Figure 6B), and wavy (Figure 6C; see Supplemental Video 2 online) root hairs. Generally, the first misshapen root hairs appeared within  $\sim 2$  to 4 h of Nod factor application. Root hair deformation occurred mainly in Zone I and Zone II (Figures 6A to 6C), whereas most of the Zone III mature root hairs remained unchanged. Typical examples of deformed root hairs, which were scored 5 h after incubation with *M. loti* Nod factors, are illustrated in Figure 6. However, no correlation was found between the altered root hair growth pattern and growth rates of root hairs. The average root hair growth rates remained approximately constant, averaging  $0.27 \pm 0.14 \mu\text{m}/\text{min}$  for Zone I and  $1.12 \pm 0.28 \mu\text{m}/\text{min}$  for Zone II root hairs. Statistical analyses clearly indicated that Nod factor application did not induce any significant changes ( $P > 0.05$ ) in the growth rates of root hairs compared with those of the control plants (Figure 2).

A quantitative comparison of cortical microtubule length and orientation after application of purified *M. loti* Nod factors is presented in Figure 7. Microtubule patterns in Zones I and III root hairs were not affected by inoculation and resembled those of control plants (Figures 7A and 7C). However, in Zone II root hairs, the population of short microtubules with a length of 1 to 10  $\mu\text{m}$  increased  $\sim 160\%$  and constituted  $>50\%$  of the total microtubule population (Figure 7A). Quantification of microtubule length and arrangement at defined distances from the root hair tip revealed that in the base part of Zone II root hairs, the length of microtubules was reduced significantly (Figure 7B) and their axial orientation was replaced by random orientation (Figure 7D). Similar alterations in microtubule length and alignment of growing root hairs were also observed after inoculation with *M. loti*, but these changes occurred slowly within 18 h of bacterial application (data not shown).

### Microtubule Dynamic Instability in Rhizobia and Nod Factor-Treated Plants

Cortical microtubules in the deformed root hairs of Lotus plants exhibited similar dynamic instability behavior (see Supplemental

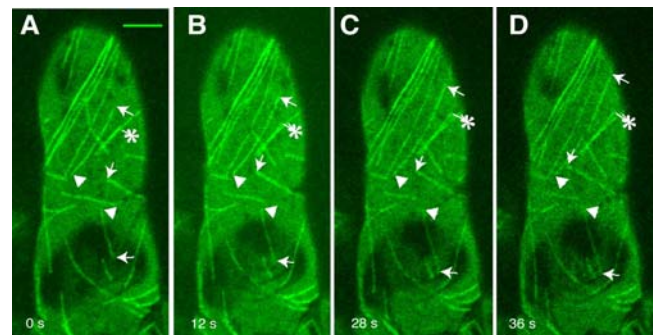


**Figure 4.** Time Series of in Vivo Dynamic Instability Behavior of Microtubules in Root Hairs of *L. japonicus*.

Arrows point to growing plus ends of microtubules, arrowheads show stable minus ends, and asterisks indicate the divergence of bundles of microtubules into fine filaments of lower fluorescence intensity. Bar = 5  $\mu\text{m}$ .

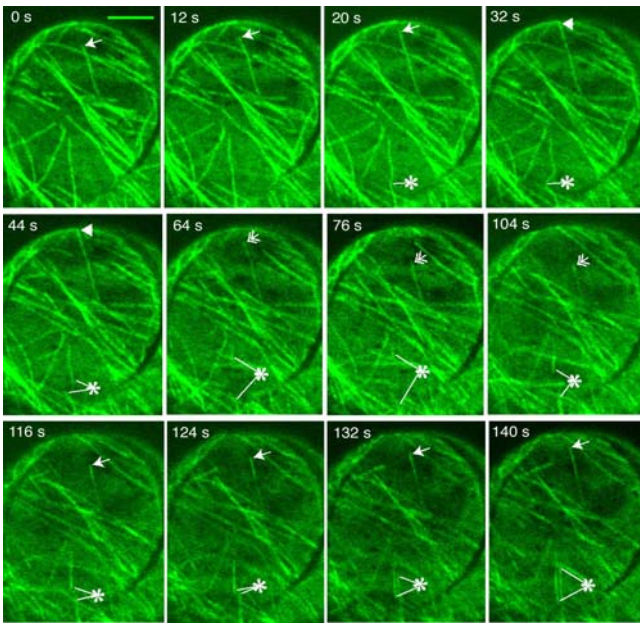


**Figure 5.** Time Series of in Vivo Dynamic Instability Behavior of a Single Microtubule in Emerging Root Hair of *L. japonicus*.

Arrows point to periods of microtubule growth (0 to 20 s and 116 to 140 s); double arrows show periods of disassembly (64 to 104 s); arrowheads indicate periods of pausing (32 to 44 s); asterisks indicate a microtubule breakage after disassembly (44 to 76 s) and polymerization (104 to 140 s) of the new formed ends. Bar = 5  $\mu\text{m}$ .

Video 2 online) to microtubules in the control uninoculated root hairs. However, plants responded to both the bacterial partner and to purified Nod factors with considerable reduction of microtubule growth rates in Zone I and Zone II root hairs (Table 1). A 46% decrease in mean microtubule growth rates was observed after inoculation with *M. loti*, and a 50% decrease was observed after application of purified *M. loti* Nod factors. These changes took  $\sim 24$  h of incubation with rhizobia (Figure 8A), whereas they occurred within 1 h of exposure to the purified Nod factors (Figure 9A). In mature root hairs, there was only slight reduction ( $\sim 20\%$ ) in growth rates of microtubules. The most significant decrease in microtubule growth rates lasted almost twice as long ( $\sim 24$  h) in bacteria-inoculated plants (Figure 8A) as in Nod factor-treated plants (Figure 9A). After 60 h of rhizobial inoculation and 18 h of Nod factor application, the differences were no longer significant. Microtubule disassembly did not show statistically significant changes after inoculation with rhizobia (Figure 8B) or treatment with Nod factors (Figure 9B), although there was a weak inhibitory effect on the average disassembly rates. However, considerable differences were found in the transition frequencies of microtubules at the time of the most dramatic inoculation-induced decreases in microtubule growth rates (Table 1). Specifically, in emerging and growing root hairs, incubation with Nod factors was associated with a 60% decrease in rescue frequency and a 40% decrease in catastrophe frequency (Table 1). A similar response pattern occurred after inoculation with rhizobia (Table 1).

## DISCUSSION

GFP-TUA6 construct of Arabidopsis was incorporated into *L. japonicus* to visualize cortical microtubule configuration in root hair cells. The insertion of the heterologous tubulin sequence did not interfere with normal plant development. Phenotypically, no differences were observed between wild-type Gifu plants and GFP-TUA6 transformants. Root hairs of transgenic Lotus plants grew at rates indistinguishable from root hairs of wild-type plants. Three of the transgenic lines generated displayed stable fluorescent labeling of cortical microtubules in root hair cells. Confocal imaging of one of the lines was used to follow the arrangement and the complex dynamic behavior of cortical microtubules throughout root hair development. We distinguished three root hair zones that correlated with their position on the root: emerging (Zone I), growing (Zone II), and mature (Zone III). The microtubule cytoskeleton coordinates many aspects of plant cell growth (Williamson, 1991), including tip growth of root hair cells (Bibikova et al., 1999; Van Bruaene et al., 2004). By studying the reaction of Arabidopsis root hairs to oryzalin, a highly effective microtubule-depolymerizing agent, Ketelaar et al. (2003) have shown that the orientation of the polarized growth of Arabidopsis root hairs depends on the entirety of the microtubule cytoskeleton. Oryzalin application leads to a visible change of the root hair growth direction.

To answer the question whether there is a relationship between microtubule arrangement and dynamics and root hair elongation, we measured growth rates of Lotus root hairs in all stages of hair cell development. The most intensive growth occurred in Zone II root hairs, whereas Zone I root hairs showed 73% lower growth rate (Figure 2). Dolan et al. (1994) have found that the development of Arabidopsis root hairs can be subdivided into two phases: an initial phase with a low growth rate (0.2 to 0.5  $\mu\text{m}/\text{min}$ ) and later phase of faster growth ( $\sim 1$  to 2.5  $\mu\text{m}/\text{min}$ ). The elongation in the first phase is attributable mainly to diffuse type of growth, but the rapid elongation in the later phase is a result of sustained tip growth. The transition from the initial slow phase to the rapid phase takes place once root hairs attain a length between 20 and 40  $\mu\text{m}$  (Dolan et al., 1994). Because the length of the emerging and short-growing root hairs in our study was between 10 and 40  $\mu\text{m}$ , the observed low growth rates in Zone I (Figure 2) were apparently associated with the diffuse-growth mechanism. The faster growth speed of Zone II root hairs was obviously a continuance of the rapid tip growth.

Time-lapse confocal imaging of microtubule dynamics in the various developmental zones of root hairs showed that plus ends of cortical microtubules were very dynamic, in that they polymerized and depolymerized rapidly (Figures 4 and 5; see Supplemental Video 1 online). Dynamic organization of microtubule arrays could be the result of dynamic instability or treadmilling polymer turnover, affecting the length of microtubules (Wadsworth, 2003). Shaw et al. (2003) have found that individual microtubules in Arabidopsis plants exhibit dynamics at both ends, undergoing slow intermittent depolymerization at the minus ends, coupled with polymerization-based dynamic instability at the plus ends. Thus, the treadmilling motility makes an important contribution to the organization of the cortical array. However, in our studies of microtubule behavior in Lotus

**Table 1.** Microtubule Dynamic Instability Parameters of *L. japonicus* Root Hair Cells

Parameters	Zone I	Zone II	Zone III
<b>Control plants</b>			
Rate ( $\mu\text{m}/\text{min}$ )			
Growth	4.62 $\pm$ 0.16	4.48 $\pm$ 0.38	3.11 $\pm$ 0.12**
Disassembly	6.84 $\pm$ 0.72	6.62 $\pm$ 0.95	6.31 $\pm$ 0.31 <sup>ns</sup>
Transition frequencies (events/min)			
Rescue	8.15 $\pm$ 2.71	7.83 $\pm$ 2.11	2.39 $\pm$ 0.22**
Catastrophe	2.14 $\pm$ 0.20	1.85 $\pm$ 0.14	1.38 $\pm$ 0.17*
<b>Plants inoculated with <i>M. loti</i></b>			
Rate ( $\mu\text{m}/\text{min}$ )			
Growth	2.50 $\pm$ 0.07**	2.41 $\pm$ 0.20**	2.49 $\pm$ 0.13*
Disassembly	6.27 $\pm$ 0.62 <sup>ns</sup>	6.22 $\pm$ 0.46 <sup>ns</sup>	6.11 $\pm$ 0.34 <sup>ns</sup>
Transition frequencies (events/min)			
Rescue	3.53 $\pm$ 1.10**	3.32 $\pm$ 0.63**	1.71 $\pm$ 0.18*
Catastrophe	1.42 $\pm$ 0.12*	1.30 $\pm$ 0.10*	0.96 $\pm$ 0.23 <sup>ns</sup>
<b>Plants inoculated with Nod factors</b>			
Rate ( $\mu\text{m}/\text{min}$ )			
Growth	2.32 $\pm$ 0.12**	2.19 $\pm$ 0.10**	2.33 $\pm$ 0.12*
Disassembly	6.23 $\pm$ 0.70 <sup>ns</sup>	6.16 $\pm$ 0.53 <sup>ns</sup>	6.08 $\pm$ 0.34 <sup>ns</sup>
Transition frequencies (events/min)			
Rescue	3.33 $\pm$ 1.22**	3.08 $\pm$ 0.51**	1.10 $\pm$ 0.12**
Catastrophe	1.30 $\pm$ 0.10*	1.14 $\pm$ 0.14*	0.83 $\pm$ 0.19*

\*\* , significant at  $P < 0.001$ , according to ANOVA; \* , significant at  $P < 0.05$ , according to ANOVA; ns, not significant at  $P = 0.05$ . Values for control Zone III root hairs were compared with those for Zone I and Zone II. Values after inoculation with *M. loti* TONO were determined from images acquired 24 to 48 h after plant inoculation and were compared with those for controls. Values after application of *M. loti* Nod factors were determined from images acquired 2 to 12 h after plant inoculation and were compared with those for controls. All values represent the means  $\pm$  SE.

root hairs, we did not find any evidence for minus end dynamics. The majority of the microtubules seemed to be anchored by their minus ends to the special initiation places (Figure 1B, asterisks; see Supplemental Video 2 online). The main functional microtubule-organizing center in plants is known to be the nuclear surface and also probably the cell cortex and the phragmoplast, where secondary nucleation sites may exist (Erhardt et al., 2002; Schmit, 2002; Shaw et al., 2003). Microtubule initiation sites in Arabidopsis root hairs are observed as discrete spots with radiating microtubules at the onset of root hair outgrowth or at the subcortex in mature root hairs (Van Bruaene et al., 2004). The same authors have found that most microtubules in Arabidopsis root hairs exhibit dynamic instability behavior at the plus ends, whereas the opposite minus ends are stable or show slow depolymerization. Our in vivo observations of cortical microtubules in Lotus root cells also demonstrated that sometimes their minus ends were released from the initiation sites, which led to microtubule depolymerization (data not shown). Obviously, the definite stability of the microtubule minus ends in Lotus root hair cells is a specific property of these cells. The microtubules anchored at their minus ends are kinetically identical to centrosomal microtubules. It is tempting to speculate that this may contribute to the overall cytoskeleton stability in the condition of acentrosomal microtubule nucleation. The releasing of the minus ends from the initiation complex may lead to the loss of microtubule stability, providing another pathway for microtubule disassembly. Thus, the cortical microtubules in

Lotus root hairs, visualized with Arabidopsis gene fusion, exhibit dynamic instability behavior at the plus ends and have quiet minus ends.

Quantification of the four standard parameters of in vivo microtubule dynamic instability revealed considerable similarity between dynamics in emerging and growing root hairs. Their microtubules exhibited higher growth rates and lower frequency of catastrophe events compared with the microtubules in mature root hairs (Table 1). A consequence of the combination of high rescue and low catastrophe frequency is that microtubule growth was almost persistent. Through the observation periods, microtubules most often grew continuously and rarely underwent a transition to the disassembly state. Dynamic instability of microtubules is considered the basic determinant of cytoskeletal reorganization allowing the microtubules to rapidly explore cytoplasmic space (Holy and Leibler, 1994). The high rescue and low catastrophe frequency may provide a mechanism by which microtubules enter the rapidly growing apical dome of root hairs. Such colonization that allows newly formed regions of cytoplasm to rapidly fill with microtubules was visualized in the tip of emerging and growing root hairs. Microtubules in mature root hairs had a rescue frequency that was  $\sim 30\%$  of that for microtubules in emerging and growing root hairs (Table 1). This finding, along with the lower microtubule growth rates in mature root hairs, is consistent with (and could explain) the decreased relative abundance of microtubules in the mature, nongrowing root hairs of Zone III (Figure 1C).

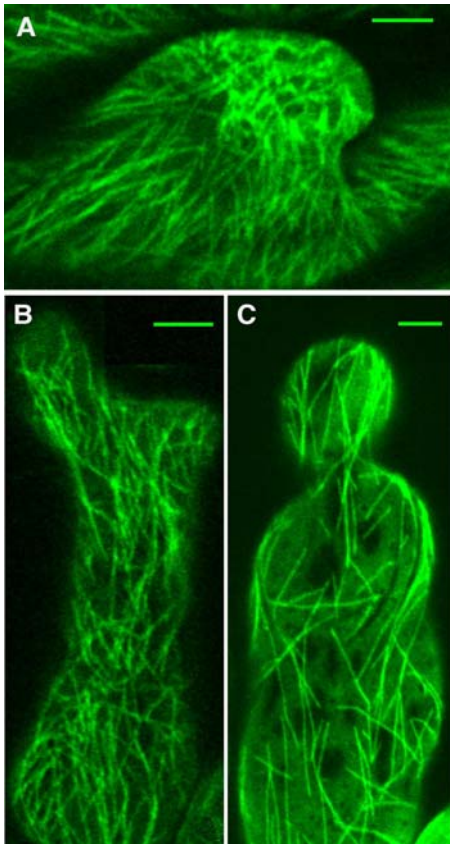


**Figure 6.** Root Hair Deformations of *L. japonicus* Plants Exposed to Purified *M. loti* Nod Factors.

(A) Emerging (Zone I) root hair at the beginning of the curling process.  
 (B) Growing (Zone II) root hair showing deformation in the form of branched root hair tip.  
 (C) Growing (Zone II) root hair displaying a waving growth pattern.  
 Bars = 5  $\mu\text{m}$ .

Taken together, the above considerations strongly suggest that the cellular mechanisms controlling root hair growth are independent of the growth dynamics of their microtubules. The average growth rates of emerging Zone I root hairs were significantly lower than the growth rates of Zone II root hairs (Figure 2), but both zones showed very similar dynamic characteristics of cortical microtubules (Table 1).

Microtubule dynamics *in vivo* change extensively in response to various regulatory signals, providing mechanisms for alterations of microtubules during specific cell events (Desai and Mitchison, 1997). The results presented here clearly indicated that the perception of symbiotic signal molecules, Nod factors, could directly affect some of the parameters of microtubule dynamic instability in root hairs (Table 1) and, thus, overall microtubule dynamics. Apart from the time frame, microtubules in root hairs inoculated with *M. loti* or purified *M. loti* Nod factors behaved very similarly. In emerging and growing root hairs, inoculation lowered microtubule growth rates by >45% and the frequency of rescue events  $\sim$ 60%. At the same time, there was no statistically significant effect on microtubule disassembly

rates. Indeed, the large decrease in rescue frequency and microtubule growth rates, combined with unchanged rates of microtubule disassembly, may reflect microtubule length and total polymer level decreasing at a specific time after symbiotic inoculation. In agreement with this suggestion is the observed increase of the population of short microtubules in growing root hairs (Figure 3B). On the other hand, the two-phase model of microtubule reorientation (Lloyd, 1994) suggests that the lifetime of microtubules depends on their orientation with respect to the cell axis. Longitudinal microtubules possess increased stability, whereas transverse-oriented microtubules are less stable and subsequently coalign into new parallel arrays. Wiesler et al. (2002) also considered the possibility of direction-dependent stability of individual microtubules and related it to tyrosination and detyrosination of  $\alpha$ -tubulin at its C terminus. In addition, Waterman-Storer and Salmon (1997) have found that specific parameters of microtubule dynamic instability in mammalian cells differ significantly depending on the location or orientation of individual microtubules. Microtubule arrangement significantly affects microtubule plus end dynamics, changing the frequency of transition events and microtubule growth and disassembly. If we consider the altered microtubule dynamics in *Lotus* root hairs in the context of these studies, it seems

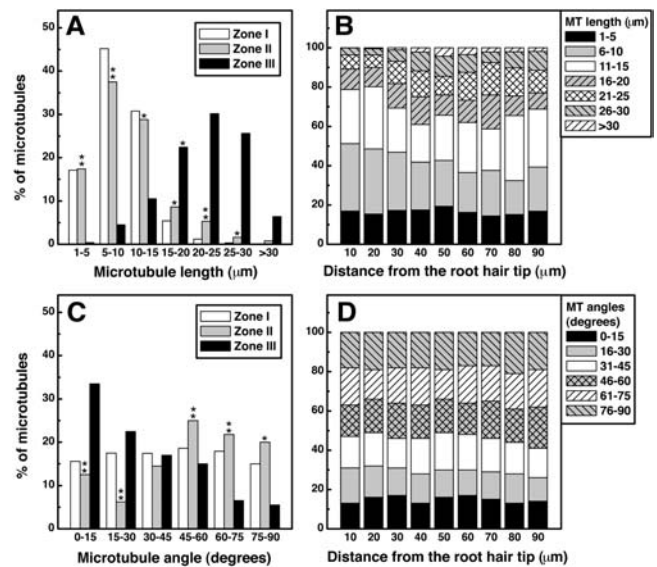


**Figure 7.** Cortical Microtubule Arrangement in Different Root Hair Zones of *L. japonicus* Plants Exposed to Purified *M. loti* Nod Factors.

(A) Average microtubule length ( $n = 1168$  microtubules from 146 root hairs).  
 (B) Microtubule (MT) length in Zone II root hairs as a function of distance from root hair tip ( $n = 450$  microtubules from 75 root hairs).  
 (C) Average microtubule angular orientation ( $n = 1185$  microtubules from 145 root hairs).  
 (D) Microtubule (MT) angular orientation in Zone II root hairs as a function of distance from root hair tip ( $n = 954$  microtubules from 106 root hairs). Double asterisks indicate a statistically significant difference at  $P < 0.001$ , and single asterisks indicate a statistically significant difference at  $P < 0.05$ , according to ANOVA. Values were compared with those for controls given in Figures 1C and 3A.

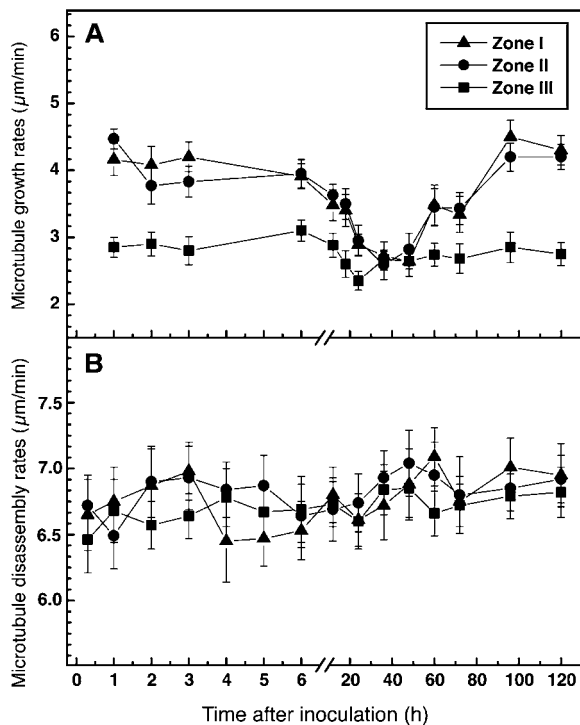


**Figure 8.** Time Course of Microtubule Growth and Disassembly Rates in *L. japonicus* Root Hairs Inoculated with *M. loti* TONO.

(A) Microtubule growth.

(B) Microtubule disassembly.

Data are averages of at least 320 microtubules measured per position from 60 to 80 root hairs. Vertical bars represent the standard errors of the means.

reasonable to suggest that Nod factor-induced alterations of microtubule orientation (Figures 7C and 7D) could affect microtubule dynamics during the course of early symbiotic interactions with rhizobia.

It should be noted that the most significant inoculation-induced decrease in microtubule growth rates was twice as long after inoculation with *M. loti* (Figure 8) than after application of purified Nod factors (Figure 9). There is a possibility that this is due to the relative chemical instability of purified Nod factors that might influence their biological activity (Perret et al., 2000). In fact, legume roots contain a variety of enzymatic activities, most likely chitinases, which rapidly degrade purified Nod factors in the host rhizosphere. The degradation products formed are only weakly active on their respective hosts (Heidstra et al., 1994; Staehelin et al., 1994).

The microtubule cytoskeleton is clearly involved in maintaining the directional control of root hair growth (Bibikova et al., 1999). During the establishment of the symbiosis, perception of the potent rhizobial signal molecule disturbs normal polarity of root hair growth, causing distortions, branching, and curling of root hairs (Long, 1996; Ridge, 1996). Application of Nod factors to Lotus plants resulted in root hair deformations that were mainly induced in the root zone containing emerging (Figure 6A) and growing (Figures 6B and 6C) root hairs, whereas the mature hairs

were not susceptible to inoculation. Nod factor-induced decrease of microtubule dynamics is thus one of the first biological responses of the host plant that precedes the visible loss of polarity of root hair cells. Consistent with this idea is the observation that microtubule dynamics were mainly reduced in emerging and growing root hairs (Table 1) that are the most probable targets of the bacterial infection (Kijne, 1992). Studies with *M. sativa* have also shown that the most responsive to Nod factor application are initiating and polar growing root hairs (Weerasinghe et al., 2003). In general, the first morphological responses of root hairs were usually noted within 1 to 3 h of Nod factor application (Heidstra et al., 1994; de Ruijter et al., 1998). Root hairs of *L. japonicus* showed the first visible alterations within 2 to 4 h of exposure to Nod factors. In most cases, these deformations followed the decrease in microtubule dynamics, suggesting that less dynamic microtubules are prerequisite for the change of the growth polarity of root hairs.

Induction of deformations by Nod factors did not alter the growth dynamics of root hairs. No significant differences could be detected in root hair growth rates of inoculated plants compared with uninoculated plants. Our data correlate with the results of Dazzo et al. (1996), who reported that clover (*Trifolium repens*) root hairs grow at a constant elongation rate (19  $\mu\text{m}/\text{h}$ ) in

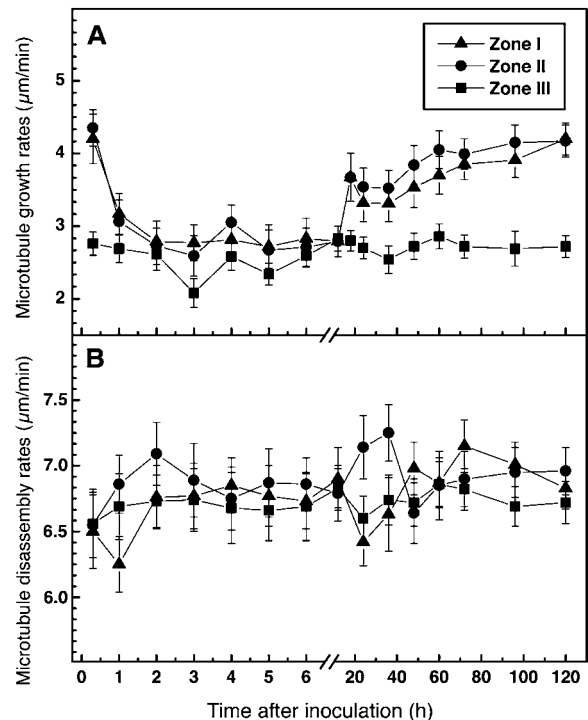


**Figure 9.** Time Course of Microtubule Growth and Disassembly Rates in *L. japonicus* Root Hairs after Application of Purified *M. loti* Nod Factors.

(A) Microtubule growth.

(B) Microtubule disassembly.

Data are averages of at least 340 microtubules measured per position from 70 to 100 root hairs. Vertical bars represent the standard errors of the means.

the presence or absence of isolated *Rhizobium leguminosarum* chitolipooligosaccharides. The observations on oryzalin-treated *M. sativa* plants have shown that this antimicrotubule drug causes depolymerization of microtubules and increases growth rates of their root hairs (Weerasinghe et al., 2003). Nod factors in combination with oryzalin increase further the length of root hairs, and microtubules disintegrate at 1 h after Nod factor exposure. These observations support the idea that microtubule disruption results in an increased root hair growth and that Nod factor application affects microtubule behavior, thereby changing the growth pattern of root hairs. However, in our *in vivo* experiments, we found no evidence of microtubule depolymerization after Nod factor treatment (Figure 6). The lasting inhibition of microtubule dynamics in Nod factor-exposed *Lotus* root hair cells (Figure 9) led mainly to change in microtubule configuration and altered the direction of tip growth (Figure 6). There is a possibility that the suppressed microtubule dynamics extends the window of root hair infectivity. A detailed microscopical investigation of root infection and nodule ontogeny in wild-type *L. japonicus* Gifu plants implies that infectivity of root hairs persists throughout their elongation development rather than just during a short period after committed epidermal differentiation (Szczyglowski et al., 1998).

In conclusion, using transgenic *L. japonicus* with GFP-TUA6 from *Arabidopsis*, we have visualized *in vivo* organization of the cortical microtubular network in root hair cells and shown that microtubules in young (emerging and growing) root hairs undergo extensive dynamic instability turnover. Quantification of the parameters of microtubule dynamic instability has allowed us to compare microtubule dynamics in different root hair zones and to find significant differences between dynamic characteristics in young and mature root hairs. We have also found that early symbiotic interactions of *Lotus* plants with *M. loti* bacteria, mediated by Nod factors, significantly changed microtubule behavior so that cortical microtubules in young root hairs became less dynamic at a specific time after symbiotic inoculation. In addition, we have shown that microtubule configuration and dynamics did not influence root hair growth rates and that the Nod factor-induced alterations in microtubule dynamics were rather prerequisite for root hair deformation. These responses of root hair cells to Nod factors reveal the details of microtubule behavior during the establishment and progression of the *Rhizobium/legume* symbiosis and provide further insight into the mechanisms of the early communication between the symbiotic partners.

## METHODS

### Transgenic Plants

A binary vector containing a fusion construct of GFP and TUA6 of *Arabidopsis thaliana* was kindly provided by T. Hashimoto (Nara Institute of Science and Technology, Nara, Japan) (Ueda et al., 1999). Transformation of *Lotus japonicus* was made according to the method described by Stiller et al. (1997). In brief, hypocotyls excised from *L. japonicus* B-129 Gifu seedlings were infected with *Agrobacterium tumefaciens* strain AGL1 harboring the above-mentioned binary vector construct. Generated calli were screened for geneticin (G418) resistance, and the regenerated plants were grown in vermiculite pots to harvest the T1

seeds. Transgenic lines with strong expression of GFP fluorescence were selected at T2 and T3 generations and used for analysis.

### Plant Growth and Inoculation

Transgenic *L. japonicus* seeds were scarified with a piece of sandpaper and surface sterilized with 2.5% sodium hypochlorite solution containing 0.02% Tween 20 for 20 min. The seeds were then rinsed with sterilized water more than six times and germinated on 1% agar plates containing half-strength Fahraeus media, pH 6.2 (Fahraeus, 1957). The plates were placed vertically to ensure the root growth along agar surface in a growth cabinet at 24°C and a light intensity of 300  $\mu\text{mol m}^{-2}\text{s}^{-1}$  (under a 16-h-light/8-h-dark photoperiod). After 3 to 4 d, seedlings with straight roots were selected and transferred to agar plates containing the same media. *Mesorhizobium loti* strain TONO (Imaizumi-Anraku et al., 1997) was grown in yeast extract-mannitol medium, pH 7.0, at 28°C. Autoclaved pieces of smooth-surface filter paper (Advantec, Tokyo, Japan) were dipped in bacterial suspension ( $10^{-6}$  cells/mL) and placed onto the agar surface. Selected 4-d-old *Lotus* seedlings were inoculated by putting them onto the surface of the inoculated filter paper. Control plants were placed on filter paper soaked in medium. At different times after inoculation, plants were removed from the plates and gently mounted in liquid culture medium, where confocal imaging on living root hair cells was done.

Nod factors were purified from *M. loti* JRL501 according to the procedures described previously (Niwa et al., 2001). The selected *Lotus* seedlings were placed on agar-coated slides with autoclaved filter paper that had been previously submerged in a  $10^{-7}$  M solution of Nod factors. Observations on treated plants were initiated 5 min after inoculation and continued over 5 d.

Root hair growth rates were calculated from length measurements taken every 10 min over a 5-d period. The length of the root hairs was determined from images acquired by an Olympus BH2 microscope (Tokyo, Japan) equipped with differential interference contrast optics and a charge-coupled device camera. Image stacks were measured using the measurement tool of ImageJ 1.30v software (National Institutes of Health, Bethesda, MD). The data were collected from randomly chosen root hairs of plants with similar root length. At least 95 root hairs were measured taken from >60 plants.

### Microtubule Dynamics: Image Acquisition and Analysis

Fluorescence imaging of root hair cells was made using a confocal laser scanning microscope (Radiance 2000; Bio-Rad, Hercules, CA) equipped with LaserSharp 4.1 software. For excitation of GFP, the 488-nm line of an argon laser was used. Confocal images were enhanced with Kalman averaging of four sequential frames. Time-lapse series, which were typically collected at 4-s intervals, lasted between 1 and 4 min. To follow single microtubules throughout the recording, the focus was manually adjusted to keep microtubules in focus. Acquired images were processed and quantitatively analyzed with NIH Image 1.62 (National Institutes of Health) and ImageJ 1.30v software by tracking the microtubule ends and using a transparent grid with printed squares placed on the computer screen. Each grid cell was proportional to an area according to the scale (size) of the source image. Growth and disassembly rates were estimated as the change in distance from the origin (the starting position of the microtubule end) versus time spent in that event. Only microtubules that had clearly distinguishable ends were used for subsequent analysis. The frequencies of catastrophe and rescue were defined as the number of catastrophic and rescue events per total time of the sequences that was acquired and analyzed. Microtubule length was determined by tracking individual microtubules using the tracking function of ImageJ 1.30v software. Because of the imaging difficulties of tracking within a bundle, mainly single microtubules, whose entire length lay within the images, were used for analysis. For comparison, the length of overlapped and

bundled microtubule structures, whose ends were not visible in the field of view, was also quantified. Microtubule angles were measured relative to the longitudinal axis of root hairs. Each series of time-lapse images was analyzed three separate times as independent sets of measurements.

All calculations and statistics were performed using KaleidaGraph version 3.6 (Synergy Software, Reading, PA). As a test for differences in the means, one-way ANOVA was used. The data are based on 21 independent experiments in which an average of 80 plants was analyzed per experiment.

## ACKNOWLEDGMENTS

We thank T. Hashimoto (Nara Institute of Technology, Nara, Japan) for providing the GFP- $\alpha$ -tubulin construct and T. Yokoyama (Tokyo University of Agriculture and Technology, Tokyo, Japan) for providing purified *M. loti* Nod factors. Our sincere thanks to Richard E. Williamson (Australian National University, Canberra, Australia) for his constructive comments on the manuscript. This work was supported by the Special Coordination Funds for Promoting Science and Technology from the Ministry of Education, Culture, Sports, Science, and Technology of Japan to H.K. and by the Postdoctoral Fellowship for Foreign Researchers from Japan Society for the Promotion of Science to V.N.V.

Received February 9, 2005; revised April 6, 2005; accepted April 7, 2005; published April 29, 2005.

## REFERENCES

- Bibikova, T.N., Blancaflor, E.B., and Gilroy, S.** (1999). Microtubules regulate tip growth and orientation in root hairs of *Arabidopsis thaliana*. *Plant J.* **17**, 657–665.
- Catoira, R., Timmers, A.C.J., Maillet, F., Galera, C., Penmetza, R.V., Cook, D., Dénarié, J., and Gough, C.** (2001). The HCL gene of *Medicago truncatula* controls *Rhizobium*-induced root hair curling. *Development* **128**, 1507–1518.
- Chalfie, M., Tu, Y., Euskirchen, G., Ward, W.W., and Prasher, D.C.** (1994). Green fluorescent protein as a marker for gene expression. *Science* **263**, 802–805.
- Cyr, R.J.** (1994). Microtubules in plant morphogenesis: Role of the cortical array. *Annu. Rev. Cell Biol.* **10**, 153–180.
- Dazzo, F.B., Orgambide, G.G., Saleela, P.-H., Hollingsworth, R.I., Ninke, K.O., and Salzwedel, J.L.** (1996). Modulation of development, growth dynamics, wall crystallinity, and infection sites in white clover root hairs by membrane chitolipooligosaccharides from *Rhizobium leguminosarum* biovar trifolii. *J. Bacteriol.* **178**, 3621–3627.
- de Ruijter, N.C.A., Rook, M.B., Bisseling, T., and Emons, A.M.C.** (1998). Lipochito-oligosaccharides with high calcium and spectrin-like antigen at the tip. *Plant J.* **13**, 341–350.
- Desai, A., and Mitchison, T.J.** (1997). Microtubule polymerization dynamics. *Annu. Rev. Cell Dev. Biol.* **13**, 83–117.
- Dhonukshe, P., and Gadella, T.W.J., Jr.** (2003). Alteration of microtubule dynamic instability during preprophase band formation revealed by yellow fluorescent protein-CLIP170 microtubule plus-end labeling. *Plant Cell* **15**, 597–611.
- Dolan, L., Duckett, C.M., Grierson, C., Linstead, P., Schneider, K., Lawson, E., Dean, C., and Roberts, K.** (1994). Clonal relationships and cell patterning in the root epidermis of *Arabidopsis*. *Development* **120**, 2465–2474.
- Erhardt, M., Stoppin-Mellet, V., Campagne, S., Canaday, J., Mutterer, J., Fabian, T., Sauter, M., Muller, T., Peter, C., Lambert, A.M., and Schmit, A.C.** (2002). The plant Spc98p homologue colocalizes with gamma-tubulin at microtubule nucleation sites and is required for microtubule nucleation. *J. Cell Sci.* **115**, 2423–2431.
- Fahraeus, G.** (1957). The infection of clover root hairs by nodule bacteria studied by a simple glass slide technique. *J. Gen. Microbiol.* **16**, 374–381.
- Goddard, R.H., Wick, S.M., Silflow, C.D., and Snustad, D.P.** (1994). Microtubule components of the plant cell cytoskeleton. *Plant Physiol.* **104**, 1–6.
- Haseloff, J., and Amos, B.** (1995). GFP in plants. *Trends Genet.* **11**, 328–329.
- Haseloff, J., Siemering, K.R., Prasher, D.C., and Hodge, S.** (1997). Removal of a cryptic intron and subcellular localization of green fluorescent protein are required to mark transgenic *Arabidopsis* plants brightly. *Proc. Natl. Acad. Sci. USA* **94**, 2122–2127.
- Heidstra, R., Geurts, R., Franssen, H., Spaik, H.P., van Kammen, A., and Bisseling, T.** (1994). Root hair deformation activity of nodulation factors and their fate on *Vicia sativa*. *Plant Physiol.* **105**, 787–797.
- Holy, T.E., and Leibler, S.** (1994). Dynamic instability of microtubules as an efficient way to search in space. *Proc. Natl. Acad. Sci. USA* **91**, 5682–5685.
- Hush, J.M., Wadsworth, P., Callaham, D.A., and Hepler, P.K.** (1994). Quantification of microtubule dynamics in living plant cells using fluorescence redistribution after photobleaching. *J. Cell Sci.* **107**, 775–784.
- Imaizumi-Anraku, H., Kawaguchi, M., Koiwa, H., Akao, S., and Syono, K.** (1997). Two ineffective-nodulating mutants of *Lotus japonicus*: Different phenotypes caused by the blockage of endocytotic bacterial release and nodule maturation. *Plant Cell Physiol.* **38**, 871–881.
- Ketelaar, T., de Ruijter, N.C.A., and Emons, A.M.C.** (2003). Unstable F-actin specifies the area and microtubule direction of cell expansion in *Arabidopsis* root hairs. *Plant Cell* **15**, 285–292.
- Kijne, J.W.** (1992). The *Rhizobium* infection process. In *Biological Nitrogen Fixation*, G. Stacey, R. Burris, and H. Evans, eds (New York: Chapman and Hall), pp. 349–398.
- Lloyd, C.W.** (1994). Why should stationary plant cells have such dynamic microtubules? *Mol. Biol. Cell* **5**, 1277–1280.
- Long, S.R.** (1996). *Rhizobium* symbiosis: Nod factors in perspective. *Plant Cell* **8**, 1885–1898.
- Margolis, R.L., and Wilson, L.** (1978). Opposite end assembly and disassembly of microtubules at steady-state in vitro. *Cell* **13**, 1–8.
- Mitchison, T., and Kirschner, M.** (1984). Dynamic instability of microtubule growth. *Nature* **312**, 237–242.
- Niwa, S., Kawaguchi, S., Imaizumi-Anraku, M.H., Chechetka, S.A., Ishizaka, M., Ikuta, A., and Kouchi, H.** (2001). Responses of a model legume *Lotus japonicus* to lipochitin oligosaccharide nodulation factors purified from *Mesorhizobium loti* JRL501. *Mol. Plant Microbe Interact.* **14**, 848–856.
- Perret, X., Staehelin, C., and Broughton, W.J.** (2000). Molecular basis of symbiotic promiscuity. *Microbiol. Mol. Biol. Rev.* **64**, 180–201.
- Ridge, R.W.** (1992). A model of legume root hair growth and *Rhizobium* infection. *Symbiosis* **14**, 359–373.
- Ridge, R.W.** (1996). Root hairs: Cell biology and development. In *The Hidden Half*, Y. Waisel, ed. (New York: Dekker Publishers), pp. 127–147.
- Ridge, R.W., and Rolfe, B.G.** (1985). *Rhizobium* sp. degradation of legume root hair cell wall at the site of infection thread origin. *Appl. Environ. Microbiol.* **50**, 717–720.
- Schmit, A.C.** (2002). Acentrosomal microtubule nucleation in higher plants. *Int. Rev. Cytol.* **220**, 257–289.
- Shaw, S.L., Kamyar, R., and Ehrhardt, D.W.** (2003). Sustained microtubule treadmilling in *Arabidopsis* cortical arrays. *Science* **300**, 1715–1718.

- Sieberer, B.J., Timmers, A.C.J., Lhuissier, F.G.P., and Emons, A.M.C.** (2002). Endoplasmic microtubules configure the subapical cytoplasm and are required for fast growth of *Medicago truncatula* root hairs. *Plant Physiol.* **130**, 977–988.
- Spaink, H.** (2000). Root nodulation and infection factors produced by rhizobial bacteria. *Annu. Rev. Microbiol.* **54**, 257–288.
- Staehein, C., Schultze, M., Kondorosi, E., Mellor, R.B., Boller, T., and Kondorosi, A.** (1994). Structural modifications in *Rhizobium meliloti* Nod factors influence their stability against hydrolysis by root chitinases. *Plant J.* **5**, 319–330.
- Stiller, J., Martirani, L., Tuppale, S., Chian, R.-J., Chiurazzi, M., and Gresshoff, P.M.** (1997). High frequency transformation and regeneration of transgenic plants in the model legume *Lotus japonicus*. *J. Exp. Bot.* **48**, 1357–1365.
- Szczyglowski, K., Shaw, R.S., Wopereis, J., Copeland, S., Humburger, D., Kasiborski, B., Dazzo, F.B., and de Bruijn, F.J.** (1998). Nodule organogenesis and symbiotic mutants of the model legume *Lotus japonicus*. *Mol. Plant Microbe Interact.* **11**, 684–697.
- Takemoto, D., Jones, D.A., and Hardham, A.R.** (2003). GFP-tagging of cell components reveals the dynamics of subcellular re-organization in response to infection of Arabidopsis by oomycete pathogens. *Plant J.* **33**, 775–792.
- Timmers, A.C.J., Auriac, M.-C., de Billy, F., and Truchet, G.** (1998). Nod factor internalization and microtubular cytoskeleton changes occur concomitantly during nodule differentiation in alfalfa. *Development* **125**, 339–349.
- Timmers, A.C.J., Auriac, M.-C., and Truchet, G.** (1999). Refined analysis of early symbiotic steps of the *Rhizobium-Medicago* interaction in relationship with microtubular cytoskeleton rearrangements. *Development* **126**, 3617–3628.
- Ueda, K., Matsuyama, T., and Hashimoto, T.** (1999). Visualization of microtubules in living cells of transgenic *Arabidopsis thaliana*. *Protoplasma* **206**, 201–206.
- Van Bruaene, N., Joss, G., and Van Oostveldt, P.** (2004). Reorganization and in vivo dynamics of microtubules during Arabidopsis root hair development. *Plant Physiol.* **136**, 3905–3919.
- Vos, J.W., Dogterom, M., and Emons, A.M.C.** (2003a). Microtubules become more dynamic but not shorter during preprophase band formation: A possible “search-and-capture” mechanism for microtubule translocation. *Cell Motil. Cytoskeleton* **38**, 278–286.
- Vos, J.W., Sieberer, B., Timmers, A.C.J., and Emons, A.M.C.** (2003b). Microtubule dynamics during preprophase band formation and the role of endoplasmic microtubules during root hair elongation. *Cell Biol. Int.* **27**, 295.
- Wade, R.H., and Hyman, A.A.** (1997). Microtubule structure and dynamics. *Curr. Opin. Cell Biol.* **9**, 12–17.
- Wadsworth, P.** (2003). Persistence pays. *Science* **300**, 1675–1677.
- Waterman-Storer, C.M., and Salmon, E.D.** (1997). Actomyosin-based retrograde flow of microtubules in the lamella of migrating epithelial cells influences microtubule dynamic instability and turnover and is associated with microtubule breakage and treadmilling. *J. Cell Biol.* **139**, 417–434.
- Weerasinghe, R.R., Collings, D.A., Johannes, E., and Allen, N.S.** (2003). The distributional changes and role of microtubules in Nod factor-challenged *Medicago sativa* root hairs. *Planta* **218**, 276–287.
- Wiesler, B., Wang, Q.-Y., and Nick, P.** (2002). The stability of cortical microtubules depends on their orientation. *Plant J.* **32**, 1023–1032.
- Williamson, R.E.** (1991). Orientation of cortical microtubules in interphase plant cells. *Int. Rev. Cytol.* **129**, 135–206.